# FIBER COIL RESONATOR FOR OPTICAL GAIN

An Undergraduate Research Scholars Thesis

by

STEVEN LAXTON

and

TYLER BRAVO

Submitted to Honors and Undergraduate Research
Texas A&M University
in partial fulfillment of the requirements for the designation as an

UNDERGRADUATE RESEARCH SCHOLAR

Approved by
Research Advisor: Dr. Madsen

May 2015

Major: Electrical Engineering

# TABLE OF CONTENTS

# ABSTRACT

Fiber Coil Resonator for Optical Gain. (May 2015)

Steven Laxton
Department of Electrical & Computer Engineering
Texas A&M University

Tyler Bravo
Department of Electrical & Computer Engineering
Texas A&M University

Research Advisor: Dr. Madsen
Department of Electrical & Computer Engineering

We have developed a cheap design for a device using 3D printed parts and simple motors to fabricate a rare earth metal doped fiber coil amplifier. We also have measurements for bending losses in a small coil and absorption of the solar spectrum in an EDFA. This research will result in the creation of a design researchers can download, 3D print, and assemble to create their own fiber coils to whatever specifications are needed. These fabricated optical devices can be used for military laser defense systems, optical concentration such as solar concentrators, microfiber resonator coils or fiber coil gyroscopes. A rare earth metal doped fiber will be tightly wrapped around an acrylic tube with no gap between rings of the coil so that when the rings are epoxied together with a similar refractive index epoxy and removed from the glass tube, it creates an effective cylinder. Because this fiber is wrapped around in many windings, a long path is created for the signal wavelength to be amplified through while the device itself is compact enough to be portable and implemented in smaller areas. This will allow for very large gain in a device that is structured to take up little space in a small volume as opposed to a cumbersome great length in a fiber many meters long.

# CHAPTER I

# INTRODUCTION

## Background

Fiber optic communication systems have come a long way since their early development in the 1970s. One of the key devices in fiber optics is the optical amplifier. Optical amplifiers allow for the direct amplification of an optical signal without converting to and from an electrical signal. The doped fiber amplifier achieves this by using interactions with rare earth metal doping ions, the most common of which is the erbium doped fiber amplifier (EDFA). With sufficient amplification, lasing occurs and the amplifier acts as a critical component of a fiber laser.

Two optical signals are coupled into an EDFA: The pump, which is meant to add power to the system, and the signal, which is meant to be amplified by the power provided by the pump. The pump is a single wavelength or a broadband source with photonic energy that is absorbed by the ions. The pump excites these ions to a higher energy level. When the photons from the signal interact with the excited erbium ions, stimulated emission occurs and the ions transfer this energy to the signal photons and relax to their lower energy state. This amplifies the signal. With a long enough line, a high enough concentration of rare earth metals and enough coupled pump power, amplification greater than the losses along the line occurs. In this instance, light amplified stimulated emission occurs, creating a higher power at the output than at the input.

Fiber optic lines are a type of cylindrical waveguide. As light travels, it is guided along the length of the line by reflection. Whenever there is an interface between the material of the

waveguide and another material, such as the outside air or a thin film layer, there is reflection and transmission that occurs as described by Snell's Law. Ideally, the pump and the signal light remain inside of the fiber by total internal reflection. Total internal reflection occurs when an electromagnetic wave reaches the boundary of the material it is being transmitted through at an angle larger than a critical angle. It can only occur when going from a material with a higher refractive index to a material with a lower refractive index, and the critical angle is found by the equation below where $\theta_c$ is the critical angle, $n_1$ is the material of the waveguide and n2 is the material it reflects off of. Furthermore, this critical angle is derived from a special case of Snell's Law where the angle of the refracted ray is 90°.

$$\theta_c = \arcsin(\frac{n_2}{n_1}) \quad (1)$$

When the ray reaches the boundary of the transmission material at an angle smaller than the critical angle, the ray splits into a reflected component and a transmitted component. The transmitted component is transmitted and lost, and that power reduction causes losses. As such, these fiber amplifiers are kept straight or wound into circles with very large radii. The smaller the radius gets, the greater the curvature of the fiber, and the smaller the angles reflecting inside the fiber get. This is called bend loss, and happens whenever a fiber is bent enough to cause total internal reflection to no longer occur.

When a fiber is bent at a constant radius to create repeated windings, a fiber coil is created. The concept of a fiber coil is a fairly new one, but has been done before for purposes such as a microfiber resonator coil. This device has its roots in the development of low-loss single-mode optical fiber developed in the 1970s for telecommunication. The microfiber resonator coil can

perform time delay, nonlinear transformation of EM waves, and sensing of ambient medium (Sumetsky). Used differently, a microfiber resonator coil can perform wavelength selective optical amplification (Arjmand, Ahmadi, Karimi).

**Theory and Application**

As material science, equipment and tools developed in the field of fiber optical communications, fiber amplifiers have increased in effectiveness. As a result, we have designed a system for winding fiber that can be cheaply assembled using 3D printed parts designed in SolidWorks, and low power stepper motors. This fabrication system allows our team to cheaply wind fiber coils ourselves for future work in developing fiber coil amplifiers for high energy laser purposes. Furthermore, we explored the concept of the fiber optic coil amplifier itself, specifically in terms of losses and gains with erbium doped fiber pumped by the solar spectrum.

The fabrication system is intended to provide automated manufacturing processes for the principle device structure – the embedded fiber coil. Accordingly, the system must be capable of forming a coil of optical fiber of arbitrary diameter, length, and pitch, and it must also be capable of embedding this coil within a thin tube of some optically favorable structural material. To keep costs low, we sought to restrict our physical design space to building assemblies out of small, 3D printable parts and standard fastener hardware, and to restrict our control methods to low power stepper motors and the Arduino microcontroller environment. A system produced to these specifications will set a lower barrier to entry for researchers to test device concepts that employ our embedded fiber coil structure.

Our fiber optic coil amplifier takes the equipment and the knowledge that has been created and gathered in the field of telecommunications and apply them to the creation of high energy lasers. Instead of using a single mode fiber for a fiber amplifier, we intend to use a dual clad fiber. The single mode fiber is useful for telecommunications as it prevents the propagations of modes other than the fundamental mode, which cuts down on noise. Since we are working with the goal of high power without transmitting information, noise does not concern us so much as loss. By using a dual clad fiber instead, we can increase the radius of the fiber, increasing the geometric cross section, and increasing the volume of the fiber. This allows for the injection of more dopant ions while more modes propagate for the pump and signal. As such we can achieve a greater gain per unit length. So long as gain per unit length is greater than loss per unit length, including the bending losses, amplification will occur.

The second change our fiber optic coil amplifier makes is by taking a one dimensional length of a fiber optical amplifier of a long length and transform it into a compact, three dimensional volume by winding it into coils. In doing so we can make a long amplifier into a compact fiber optic coil amplifier that can be transported easily and is convenient to work with as well as fits into small spaces. Since the amplifier is being bent into these windings there is a bend loss in place, but with the large number of windings such a long distance worth of gain can be created that it exceeds the bend losses.

This fiber optic coil amplifier will therefore be similar to a compact cylinder composed of several windings of a rare earth metal doped fiber. Using a side coupling mechanism, a large amount of pump power can be coupled into the fiber optic coil amplifier for high amplification.

# CHAPTER II

# METHODS

## Fabrication

Automated fabrication of the embedded fiber coil consists of two macroscopic design objectives: Wind bare fiber into a coil of constant pitch, and embed this coil within an optically transparent structural tube. This is to say, bare fiber must be coiled to a certain specification with a measurable degree of precision, and the resulting coil must be embedded within some optically favorable structural material. Our fabrication system handles these tasks in parallel by reeling tensed fiber about an acrylic spindle, and simultaneously applying and curing a UV curable optical adhesive between newly created windings. Physical manipulation of the fiber is handled by a system of stepper motor driven 3D printed assemblies, and control over each of these steppers is provided by an Arduino UNO microcontroller board. The steppers employed are small 5V units from Kiatronics (28BYJ-48).

## Stripping

Device specification calls for an embedded coil of bare optical fiber. Prior to any automated fabrication system coiling procedures, an appropriate length of the fiber-to-be-coiled must be stripped of its protective coating. The coils are of centimeter scale length and diameter, so the required length of bare fiber is on the order of tens of meters. Equation 2 can be used to approximate the length of fiber necessary for a coil of arbitrary height ($h_{coil}$) and minor coil radius ($R_{spindle}$), and of any number of layers ($L$).

$$l_{fiber} = \sum_{n=0}^{L-1} \frac{2\pi\left[R_{spindle} + R_{fiber}(1+2n)\right]}{2 * R_{fiber}} * h_{coil} \quad (2)$$

As an example, the length of standard single mode fiber required for a single layer, one inch long coil (2.54 cm) around a 1.6 cm radius spindle is approximately 10.25 meters. These long lengths of bare fiber necessitate a stripping process that is tolerably gentle and practically efficient in time, and that also safely packages the resulting fiber for the processes that follow.

To satisfy these requirements, an acid stripping method was used to iteratively strip and store one meter of the fiber-to-be-coiled. Procedurally, a one meter section of fiber is stripped by the appropriate sequence of chemical baths, then is wound about a large radius temporary storage spool that is used to feed the coiling system. The next meter undergoes the same process, and it continues until the desired length is stripped. Finishing the job, the fiber is clipped from the main spool and fastened to the temporary spool. It should be noted that a workable length of coated fiber is left on each end of the fiber-to-be-coiled for the purpose of providing protected leads to the embedded fiber structure that results.

**Automated Fabrication System**

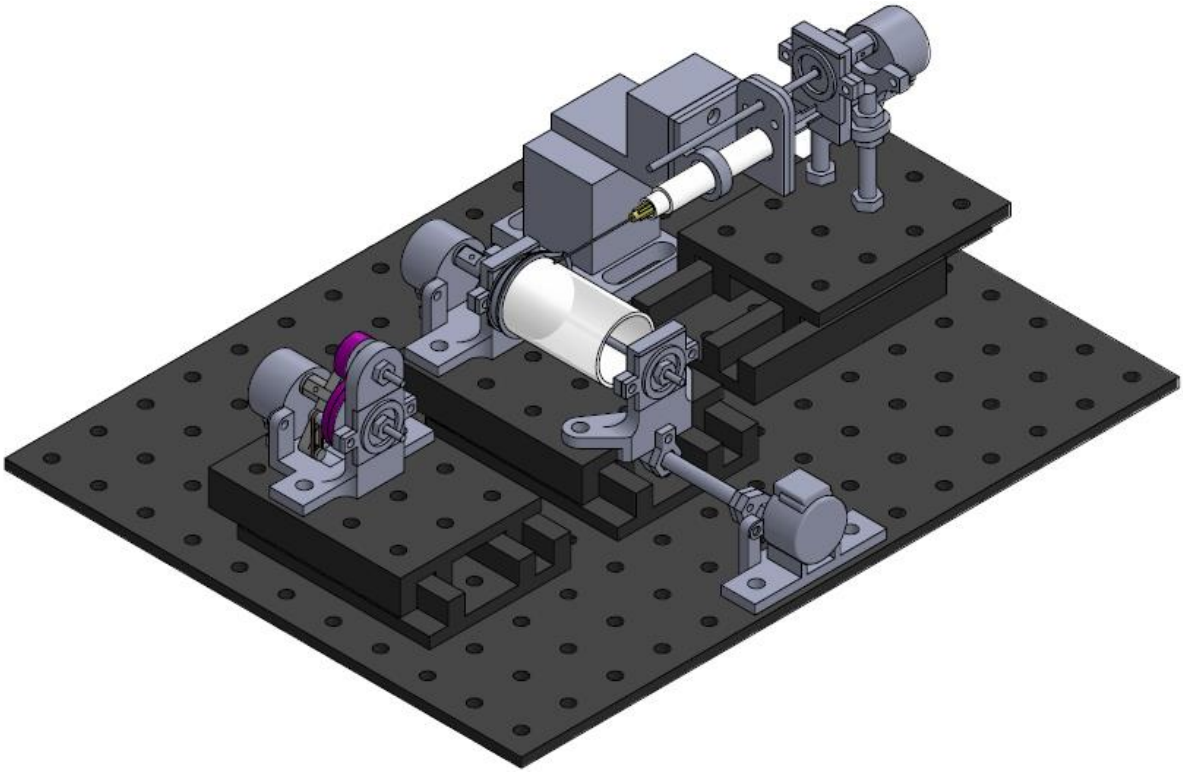

**Figure 1: Automated Fabrication System (AFS) Overview**

The automated fabrication system (AFS) consists of four principle devices, each driven by an Arduino UNO controlled stepper motor. As depicted in figure 1, these are the winding, tensioning, translating, and epoxying devices. In principle, the winding device will pull fiber from a fixed point on the tensioning device by reeling it around an acrylic spindle. While it reels in more fiber, the winding device will be translated axially by the nut-and-bolt linear actuator scheme of the translating device. By this method, the translating device's stepper provides a control for the pitch of the coil being reeled in. As the coil begins to take shape on the spindle, the epoxying device will deposit a controllable volume of UV curable epoxy in the gaps between each fiber wind, and this epoxy will be cured a short rotation from the deposition point.

In what follows, the two basic processes of the AFS – creating the coil, and epoxying the coil – will be stepped through in a manner that allows the specific features and operating principles of

each device to be discussed in detail. Equations for determining relative stepper speeds for an ideal, zero gap coil will also be presented. Finally, the initialization protocol for using the AFS to manufacture an embedded fiber coil will be established.

*Coiling Process*

The coiling process of the AFS operates on the principles of a reeling mechanism, whereby a length of un-tensed fiber is pulled in by the system and wound helically around the acrylic spindle. To achieve this reeling mechanism, the AFS needs to provide solutions for three constituent methods. First, it needs to provide a method for the tip of the fiber to be fixed directly to a stably rotating spindle assembly. This allows fiber to be 'pulled in' and wrapped around the spindle, but it relies on there being some element of tension in the fiber to keep the windings from coming undone. The second method is thus an active tensioning routine that is capable of imparting tension to the un-tensed fiber, before it is pulled to the spindle. The tensioning device fulfills exactly this purpose. The third method is one that allows the rotating spindle to be translated axially. Since the tensioner provides a static point from which the winder pulls fiber, translating the spindle axially will provide a mechanism for controlling the pitch of the coil. These three methods are discussed in detail below.

Fiber Fixing Method

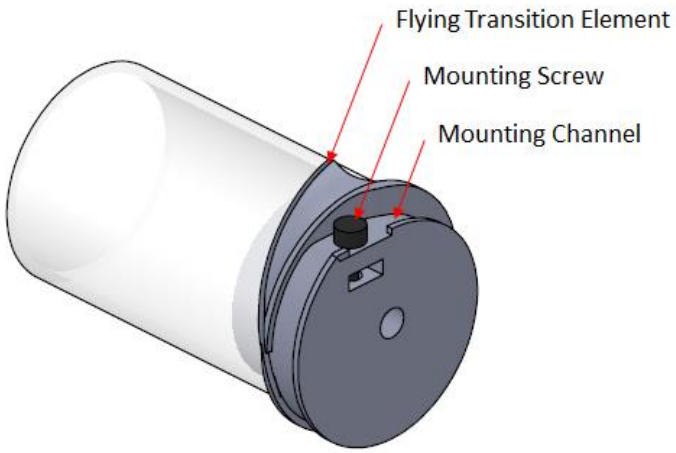


**Figure 2: Spindle Assembly**

The rotating spindle assembly is pictured in figure 2. It consists of the 3d printed spindle mount, and the acrylic spindle itself. The spindle mount serves to connect the acrylic spindle to the stepper's rotating axle, and was also designed with a feature that allows fiber to be easily hard mounted then fed to the spindle. Following the definitions of figure 2, the tip of a fiber can be fixed between the spindle mount and the head of the mounting screw. The fiber can then be wound around the mounting groove and fed into the spindle mount's flying transition element. The flying transition element allows the fiber coil to be started an appreciable distance away from the edge of the acrylic spindle, and it also allows that the acrylic spindle need not have a perfectly flat end face. That the spindle need not have a flat end face simplifies the manufacture of the spindles, as less care needs to be taken when cutting segments from the initial acrylic tube. With a fiber securely fastened to the spindle mount and laid in the flying transition element, the necessary procedures to initialize the tensioning device can begin.

Active Tensioning Method

For the winding device to effectively reel in optical fiber, it is required that there is some force constantly working to counteract the fiber's tendency to return to its un-bent state. With respect to the coiling system, this tendency corresponds to the unravelling of the coil. The tensioning device is thus employed to impart a stable element of tension along the length of fiber spanning the two devices. Given that the tensioner must also continuously feed new fiber to the winder, the solution is slightly more nuanced than might be expected.

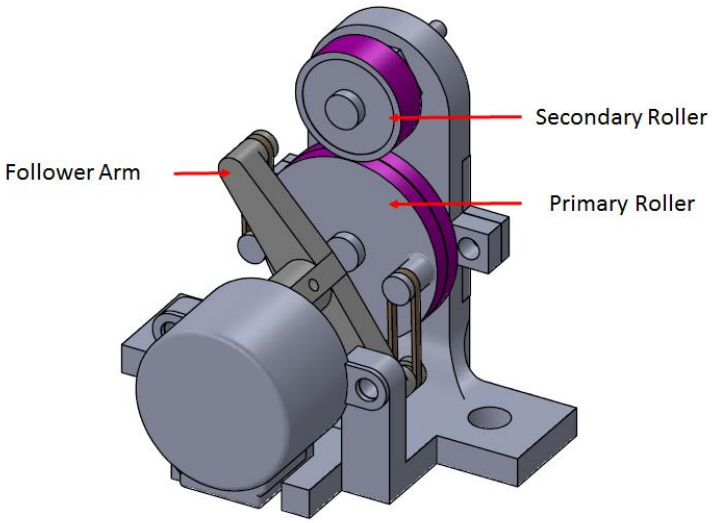


**Figure 3: Tensioning Device**

The tensioning device is pictured in figure 3. The parts principally related to the active tensioning method are the primary and secondary rollers, and the stepper-controlled follower arm. The rollers are two ball-bearing based, low friction rollers, mounted such that there are compressive forces exerted on an optical fiber that passes between them. This compression provides forces that are normal to the fiber to roller interfaces, thus contributing to the amount of static friction at these interfaces. To further augment the gripping potential of the rollers on the

fiber, each is wrapped with cuts from the fingers of standard, disposable nitrile lab gloves, effectively increasing their coefficient of static friction.

Given this mechanical relationship, the act of pulling a fiber between the rollers will cause both to rotate with limited slip at the fiber to roller interfaces. Since the rotating action of these rollers is low friction by design, a secondary mechanism acting on the rollers is required to impart tension to the fiber. It is clear that even if the rollers provided tension through some internal kinetic friction, the passive nature of this tension would introduce difficulties when trying to automate winding and unwinding processes.

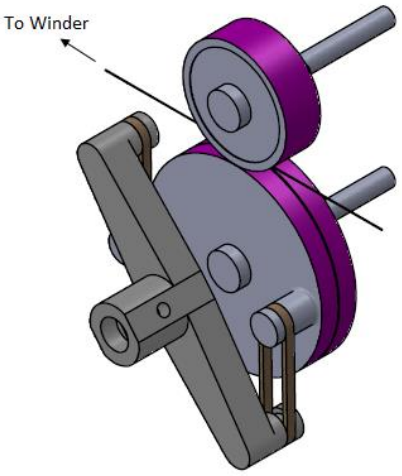


**Figure 4: Principally active parts on the Tensioning Device**

Thus to actively introduce tension, rubber bands are mounted to pegs on the primary roller, and stretch to pegs on the stepper mounted follower arm. Following figure 4, if fiber is pulled through the rollers by the winding device, the primary roller will rotate with some constant

angular velocity in the counter-clockwise direction. If at the same time the stepper mounted follower arm remains static, the limited slip design of the fiber to roller interfaces will allow tension to build in the fiber as the primary roller rotates and stretches the rubber bands. It follows that if at some stretched length the winding device stops pulling in new fiber, there will be a constant element of tension in the rubber bands. Even in motion, any static level of stretching on the rubber bands will impart a constant tension to the fiber, therefore if the follower arm is made to rotate with the same angular velocity that the winder imparts to the primary roller, a constant element of tension can be passed to the reeling fiber.

Since the angular velocity of the primary roller is determined by the angular velocity of the acrylic spindle, a relationship between the angular velocities of the winding and tensioning steppers can be derived that ensures the constant tension condition. This equation is given below, with ($R_{PR}$) as the primary roller radius.

$$\omega_{tensioner} = \frac{R_{spindle}}{R_{PR}} \omega_{winder} \tag{3}$$

For our system, the primary roller radius is equal to the acrylic spindle radius, therefore both steppers rotate at the same RPM.

Translation Method

The tensioning device feeds the winding device from fixed location that is perpendicular to some point along the acrylic spindle's axle. To control the relative location of the feed point with respect to the spindle's axle, the translating device employs a nut-and-bolt linear actuator to

finely control the low friction translating stage that the winding device is mounted to. A nut is firmly embedded in the winding device's secondary axle tower, and its corresponding bolt is firmly attached to the off-stage, statically mounted translator stepper. As the stepper drives the bolt through the nut, the translating stage is linearly actuated.

Ideally, the embedded fiber structure will consist of a fiber coil with zero space between each individual winding. Said another way, the pitch of the coil should be equal to the diameter of the fiber being coiled. Given this condition, and given the threads per unit length of the actuated bolt, a relationship between the angular velocities of the translating and winding steppers can be established. Equation 4, below, is this relationship, with (TPL) as threads per unit length of the actuator bolt, and ($D_{fiber}$) as the diameter of the fiber being wound.

$$\omega_{translator} = TPL * D_{fiber} * \omega_{winder} \quad (4)$$

*Epoxying Process*

Rather than form a complete coil, then subject the coil to some epoxying procedure, the AFS accomplishes both tasks simultaneously by using a 'groove beading' epoxy method. Groove beading refers to the manner in which epoxy is deposited onto the coil – as the coil is wound, the epoxying device actuates a syringe at a specific rate, such that the appropriate volume of epoxy is beaded into the groove between each newly created wind. After being deposited in this groove, the epoxy will rotate with the spindle into the exposure region of a UV source, thereby curing the epoxy and forming the structural tube. This method relies heavily on proper alignment and a controllable rate of epoxy discharge, which the AFS readily provides solutions for.

Groove Beading Method

Alignment to the groove is greatly simplified by the spindle translation method of the coiling process. Given that the tensioner feeds fiber from a fixed point that is perpendicular to the spindle axle, fiber will always be pulled onto the spindle at the same absolute position, as in figure 5. As a result, full process alignment can be achieved by initializing the position of the syringe tip above the principle groove.

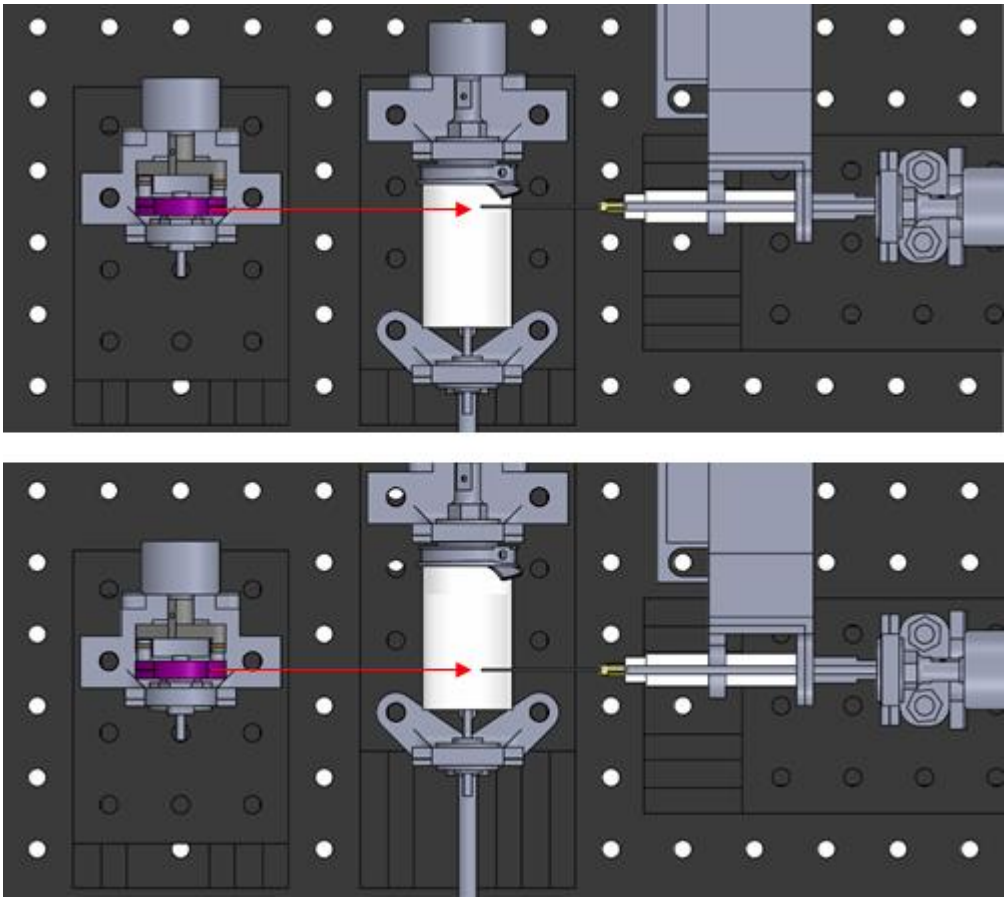

**Figure 5: Alignment mechanism of the groove beading method. Since the tensioning and epoxying devices are statically mounted, alignment is maintained throughout a coiling procedure.**

To align the tip of the syringe with this principle groove, the epoxying device provides manual translation controls in the directions perpendicular to the spindle axis. Using these controls, the tip of the syringe can be moved to a specific radius and angle relative to the spindle axis that is

determined to be ideal. An ideal position would be one that deposits epoxy in the groove at the same volumetric rate that the syringe extrudes it. The tensioning device completes the alignment procedure by providing manual translation controls parallel to the spindle axis. Using these controls, the fixed feed point of the translator can be moved laterally such that the principle groove lies directly beneath the tip of the syringe.

After principle groove alignment has been established and the AFS begins its automated process, the epoxying device uses a stepper controlled nut-and-bolt actuation scheme to drive the syringe plunger at a constant rate, thus extruding a constant volume per unit time from the syringe tip. Truly though, the actuation does not provide the force that extrudes the epoxy. Since the thick epoxy would require a significant amount of torque to be extruded, the plunging duties are re-assigned to the spring loaded translating stage that the motor carriage is mounted to. In this sense, the actuation of the screw serves only serves to allow the stage spring to drive the plunger.

To determine a satisfactory rotation speed for the syringe stepper, equation 5 returns the syringe stepper speed necessary for extruding a differential volume that is 'N' times the area of the fiber being coiled. In this sense, an ideal value for N would be 0.1366, which corresponds to exactly the area of the groove's cross section. Other notable terms in the equation are ($R_{tube}$), which is the minor radius of the syringe tube, and (TPL), which is the threads per unite length of the actuated bolt. As the operational equation is not particularly intuitive, a short derivation is provided.

$$dV_{syringe} = A_{tube} * dl_{actuated} \qquad dV_{spindle} = N * A_{fiber} * dl_{rotated}$$

$$dV_{syringe} = \pi R_{tube}^2 * \frac{d\theta_{syringe}}{TPL*2\pi} \qquad dV_{spindle} = N * \pi R_{fiber}^2 * \left(R_{spindle} + R_{fiber}\right) d\theta_{\text{spindle}}$$

$$\frac{dV_{syringe}}{dt} = \frac{dV_{spindle}}{dt}$$

$$\omega_{syringe} = N * 2\pi \left(\frac{R_{fiber}}{R_{tube}}\right)^2 * TPL * (R_{spindle} + R_{fiber}) * \omega_{winder} \tag{5}$$

An AFS manufacturing process will also require a UV source to cure the deposited epoxy. The specific setup of the UV curing source has not yet been established, but the setup will require that the yet-to-be-deposited epoxy in the syringe tube be adequately shielded from exposure. This will likely be accomplished with aluminum foil. With respect to creating a correctly positioned UV exposure region, a bundle of optical fiber may be employed to offer a less intrusive and more precise solution than simply pointing the source at the side of the spindle.

*Initialization Protocol*

Before the AFS can begin its automated processes, the fiber must be properly inserted into the system, and the syringe needle must be properly aligned for the groove beading method. To avoid damage to certain AFS parts or to the fiber itself, these tasks must be completed in a particular order, and in a particular manner. This initialization protocol is described in the following paragraphs.

Before any interactions with the AFS, the fiber tail intended to be held by the fiber fixing mechanism must maintain at least 40cm of protective coating. This will provide enough coated

fiber loops on the acrylic spindle for the syringe needle to be placed over the principle groove without contacting the flying transition element.

To load the fiber into the AFS, the rubber bands should be removed from the tensioning device, and the coated tip passed through the rollers. The fiber can then be pulled through the rollers so the tip may be fixed to the spindle mount using the mounting screw. After fixing the fiber, the rubber bands should be re-attached to the tensioning device, and the follower arm positioned such that tension develops in the fiber.

With the fiber hard mounted to the spindle mount and tensed by the tensioner, an Arduino routine that drives the spindle stepper and tensioner stepper for constant fiber tension (equation 3) should be run for a single rotation of the spindle. During this routine, the fiber should be manually guided around the spindle mount and on to the flying transition element. After this single rotation, the fiber should come to rest on the surface of acrylic spindle.

While the fiber is on the surface of the spindle, it will likely not follow an axially perpendicular path from spindle to tensioner. To establish this condition, Arduino routines that incrementally rotate the translator stepper should be executed. Once perpendicularity is achieved, a coiling routine established by the tensioning and translating equations can be run until the coated-to-stripped transition on the fiber reaches the surface of the spindle. These are equations 3 and 4, respectively.

Next, the syringe needle can be translated by the epoxy system to the desired location above the surface of the coil. Now at the correct radial location, the needle can be laterally aligned with the principle groove by simultaneously translating the acrylic tube and tensioner. Once this alignment is achieved, the UV curing source is properly positioned, and the appropriate shielding measures are taken for the epoxy supply in the syringe, the AFS can begin executing its embedded fiber coil manufacturing routine.

**Measurements**

Two experiments were designed to get two preliminary. Both experiments follow a very similar setup. One is designed to get the measurements for losses caused by various numbers of windings. The other is designed to measure the pump absorption, which stimulates rare earth metal ions to create gain, across the solar spectrum.

Below is the general experimental setup for both experiments.

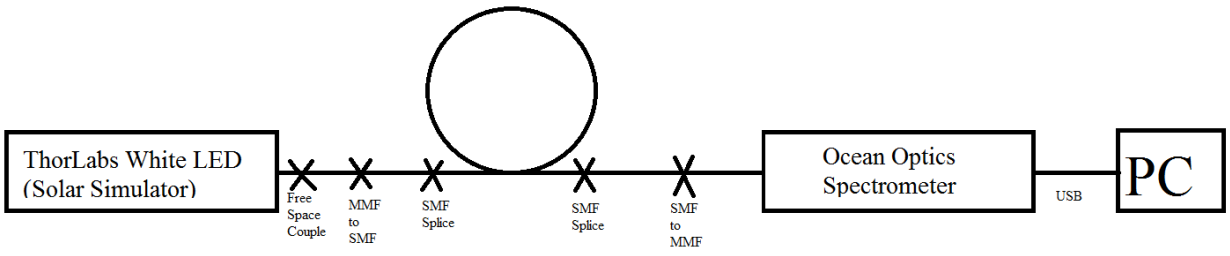


**Figure 6: General Experimental Setup**

At the first input is a ThorLabs White LED. The light that the LED emits simulates the broadband solar spectrum. At the output of the LED is a free space couple into the input of a multimode fiber. This multimode fiber guides a portion of the light to its output, where there is a

metal connector to a single mode fiber. There is notable loss at this couple, which is by design: with too much power coupled directly into the single mode fiber, the fiber can become damaged. This single mode fiber is then spliced to the single mode fiber device under test, which differs between experiments. The device under test is also spliced to another single mode fiber, which is mechanically connected to another multimode fiber. This multimode fiber is mechanically connected to an Ocean Optics Spectrometer. This spectrometer measures the absolute irradiance at every wavelength across the spectrum, and sends the data to a PC with software for analysis.

For the device under test in the absorption experiment, pairs of single mode fiber were cut and spliced to the single mode fiber ends. One part of the pair is an undoped single mode fiber used as reference. The other part of the pair is an erbium doped single mode fiber. Pairs were created at various lengths: 10cm, 22cm, 44cm, 70cm, and 90cm.

First, the doped fiber was connected for absolute irradiance testing. Then, the undoped fiber, which acts as a reference, was connected for absolute irradiance testing. Since both devices were connected under the same experimental setup, with the same lengths, the losses due to the connections and lengths are the same. Only one other loss should occur, and that is due to absorption of the light by the rare earth metal ions.

By taking the measurement of the absolute irradiance of the doped fiber, dividing it by the measurement of the reference fiber, and putting that fraction in the argument of log base ten we find only the loss in dB caused the absorption as other losses are cancelled out by the division.

Then, by multiplying a negative, we turn the negative dB into a positive dB to describe it as positive absorption. The equation used is below:

$$Absorption = -10LOG10\left(\frac{AI_{doped}}{AI_{ref}}\right) \quad (6)$$

The second experiment uses this equation as well, except to measure loss caused by winding as opposed to absorption.

In the second experiment, the device under test is a six meter long single mode fiber with the absolute irradiance measurements made when it is straight, as a reference, and when it is wrapped around our acrylic cylinder base with different numbers of winds. In the same way all losses except absorption were cancelled for the first experiment, all losses except those caused by the windings are cancelled for this experiment. Measurements were made with one wind, five winds, ten winds and fifteen winds.

*Coupling*

The last experiment only made it to the qualitative stage as is not a primary component of our research. This experiment was done the answer the question if the pump light could be coupled into the device by a side insertion method that takes advantage of the structure of the device.

With the coil tightly wound, the structure creates a thick shell hollow cylindrical shape. If light is coupled tangentially to the surface of the coil, that is, 90° from the normal to the cylinder, a wide

angle is produced by the refraction with the air-cylinder interface that allows for close to total internal reflection.

In this experiment, a purple laser pointer was activated and pointed at the acrylic cylinder base, which has close to the same internal and external radius of our coil, at various angles including perpendicular and tangential. If the acrylic cylinder fluoresces and there is a decrease in the amount of light outside of the cylinder, then it can be inferred coupling has occurred. The fluorescence itself is caused by imperfections inside the acrylic cylinder, but it shows that light was coupled into the cylinder in order to be fluoresced by the imperfections.

# CHAPTER III

# RESULTS

## Embedded Fiber Coil

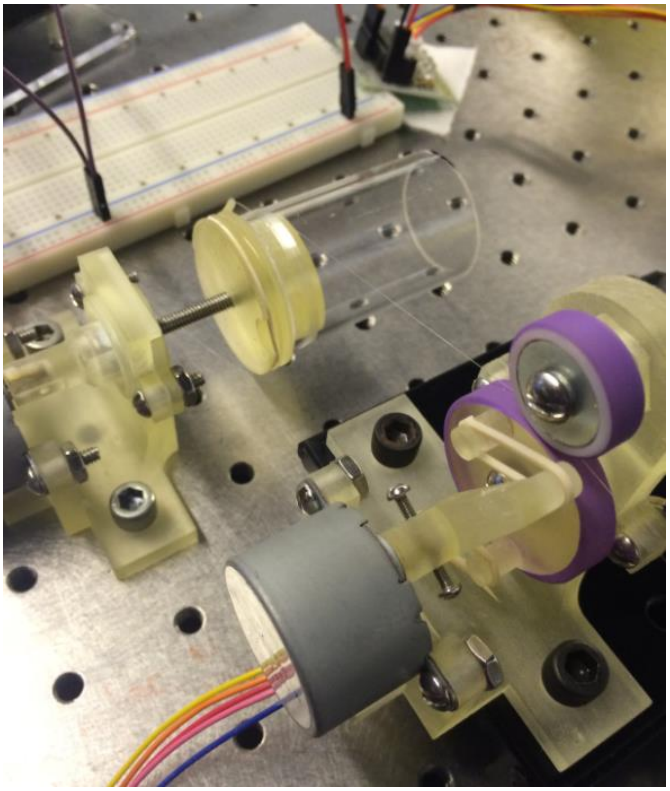

**Figure 7: Early build of the Automated Fabrication System**

A preliminary manufacturing result was achieved from an early build of the automated fabrication system (AFS). The build in question is pictured in figure 6, and consists of a single axle tower winding device with a rubber band based fiber fixing method, a tensioning device of the same variety as the final build, and a translating device that actuates the tensioning device rather than the winding device. No epoxying device had been fabricated at this point, so in effect this was a test of the AFS's coiling process. Using this version of the AFS, we were able to

automatically wind more than 20 coils of mechanically stripped fiber around the acrylic spindle, as well as manually confirm the concept of using UV curable epoxy as a structural material.

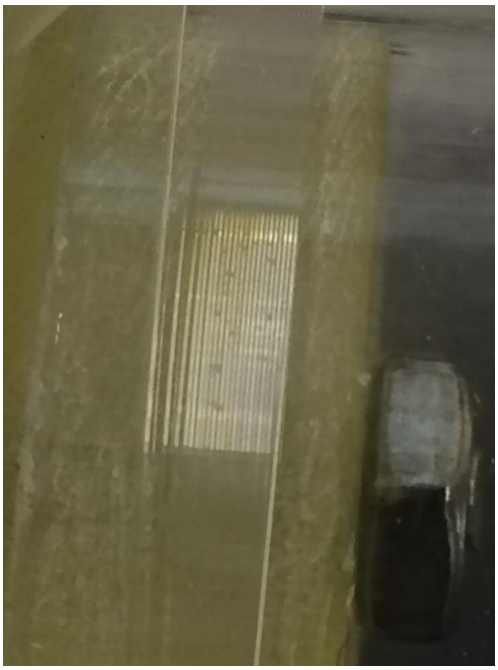

**Figure 8: Close up capture of a 22-wind coil resting on the acrylic spindle.**

Figure 7 shows a close up image of one of the coils produced using the early build's automated coiling process. This specific coil contains 22 winds of mechanically stripped, standard single mode fiber. The mechanical stripping process limited the number of winds on our test coils, as the process was time inefficient and required too much manual dexterity to safely handle the fiber during stripping and cleaning. The acid stripping method could have been used were it available, but that this result was achieved from mechanically stripped fiber may be more of a testament to the fiber processing capabilities of the AFS.

From repeated tests of this build's automated coiling process, we observed that the winding, tensioning, and translating device setup was capable of reliably producing coils of uniform and

controllable pitch. This was in spite of the single axle tower configuration and its wobbly bearing, which had a tendency to transmit off-axis rotation to the spindle assembly. To combat this off-axis rotation, later builds would incorporate a second axle tower to support both ends of the spindle assembly's axle. It was planned that this second axle tower would allow perfectly axial rotation despite the low quality, wobbly bearings embedded within them. Higher quality, lower friction bearings are also being taken into consideration to further improve performance.

A second change that resulted from these tests was a more reliable and efficient fiber fixing method for the spindle mount. The rubber band method of this early build was cumbersome to use and did not always produce the same compressive holding force on the fiber, causing the initialization process to be unreasonably difficult. By exchanging the rubber band based compressive force for a fastener based compressive force, the fiber fixing method became much more straightforward to use.

In figure 8, the concept of an epoxy embedded fiber coil is demonstrated. The left image is of a dual-tailed, self-supporting fiber coil held together by manually applied epoxy. The right image is of the same coil but with demonstrably more epoxy, and was captured after a handling error caused part of the coil to splinter, resulting in the loss of one of the fiber tails.

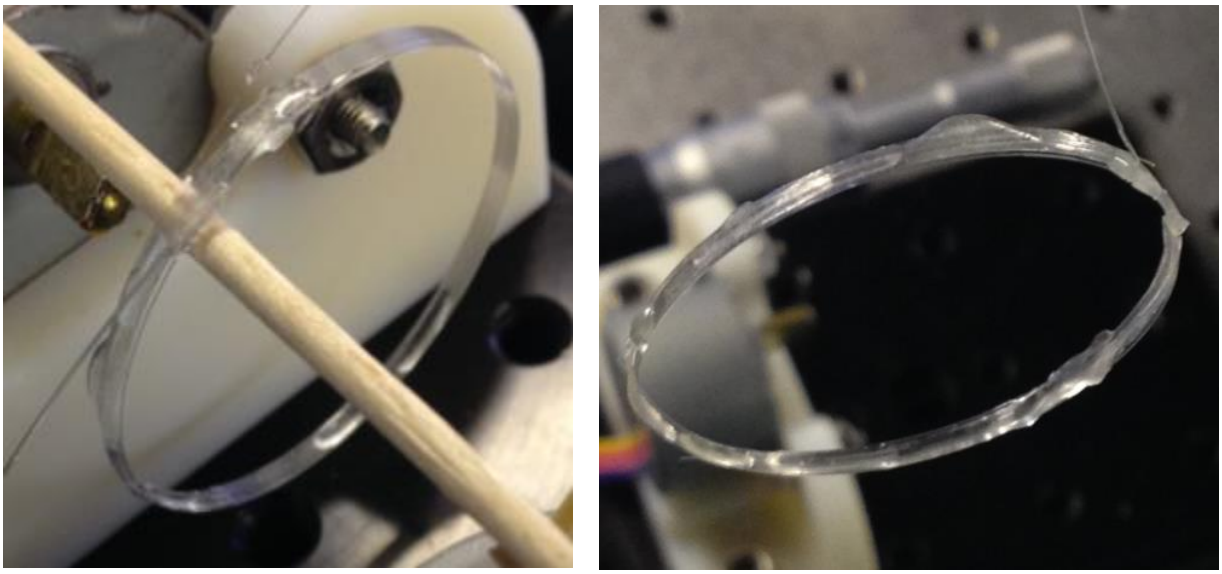

**Figure 9: Images of a manually epoxied, self-supporting fiber coil.**

The epoxy used to bind the coil in figure 8 was a general purpose, UV curable optical adhesive from Norland (NOA68). This epoxy has a cured index of refraction of approximately 1.56, which is non-ideal for achieving the desired optical properties of the embedded fiber device, but is satisfactory for the purpose of confirming structural concepts. At the time of manufacture there was no epoxying capabilities built into the AFS, so the epoxy was manually applied with a dropper after the AFS created a 13 wind stripped coil. Procedurally, epoxy was dripped on top of the coil and allowed to diffuse for a short time before being exposed by a UV source. The spindle was rotated, and this process repeated until the whole coil was embedded in cured epoxy. Removing the coil from the acrylic spindle proved simple despite over deposition of adhesive, as the adhesive was poor at bonding to the acrylic spindle. The final build of the AFS will ideally have no over deposition, as the groove beading method, combined with a zero gap coil, will severely limit the amount of epoxy that contacts the spindle.

**Automated Fabrication System Assembly**

Time constraints restrict us from reporting on the embedded fiber coil manufacturing capabilities of the full AFS. Even so, the full system has been assembled, so we are at least able to report our findings related to the mechanical behavior of certain features. An image of the assembled AFS is given in figure 9.

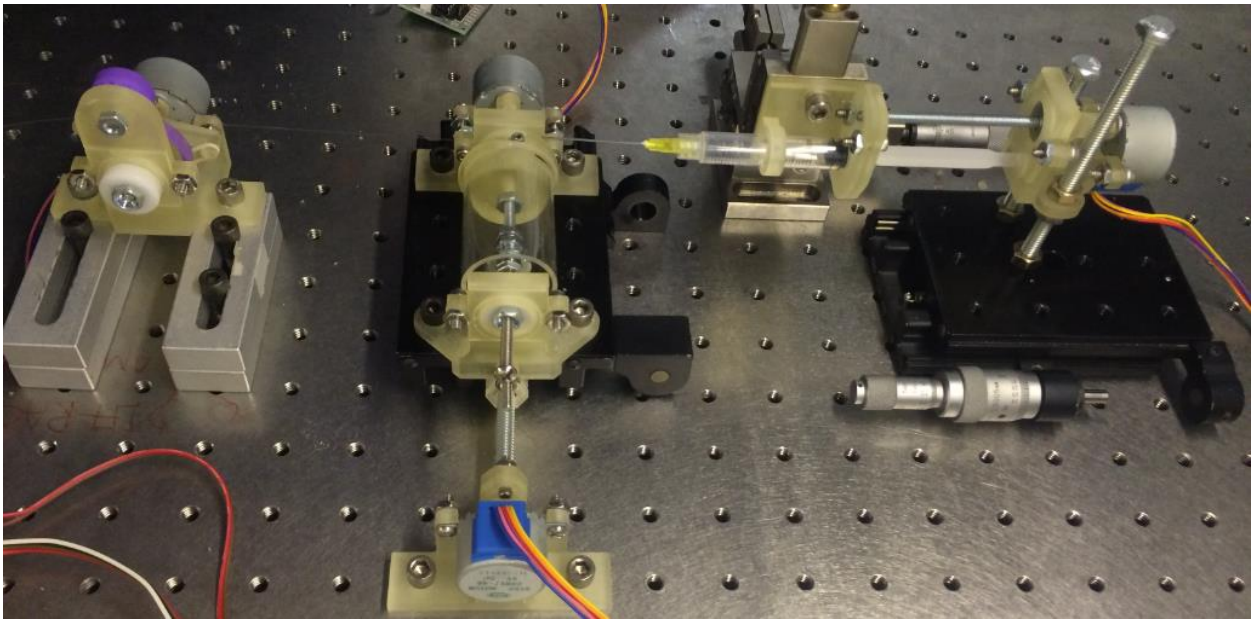

**Figure 10: Overview of the mechanically assembled Automated Fabrication System**

Principle among features to test on the final build of the AFS was the fastener based fiber fixing method on the spindle mount. We found that the fastener based method was very easy to use, provided plenty of holding power, and was also gentle enough that the fiber did not break under the compressive stress. Figure 10 is a close up capture of the winding device, and with some strain it can be seen that the tip of a fiber is clamped by the fastener. The fiber wraps around the spindle mount and up the flying transition element, then feeds into the tensioner, which we can also observe is successfully imparting tension to the fiber.

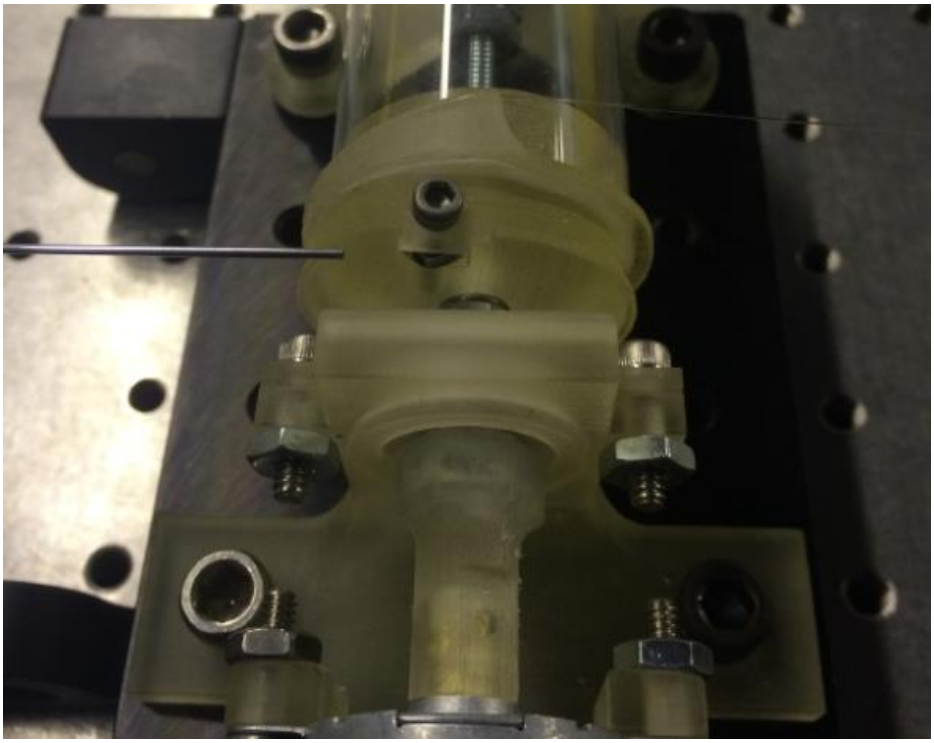

**Figure 11: Operational fiber fixing method.**

Next, the spindle assembly was tested for perfectly axial rotation, but the results come with an asterisk. The appropriate hardware could not be sourced for the axle – the machine screws we had access to were too short to span the gap between the axle towers – so our results are based on a makeshift screw coupler made out of re-purposed hardware, as in figure 11. The rotation was decidedly off axis, but we believe it is due to very short length-scale of the coupler – the weight of the spindle assembly caused the axle to sag at the coupler. An appropriately sized axle screw, or a longer and purpose built screw coupler will be required to determine the real results of this test. If off-axis rotation persists, it will likely be a result of the low quality bearings used in the axle towers, so higher quality bearings may need to be sourced as well.

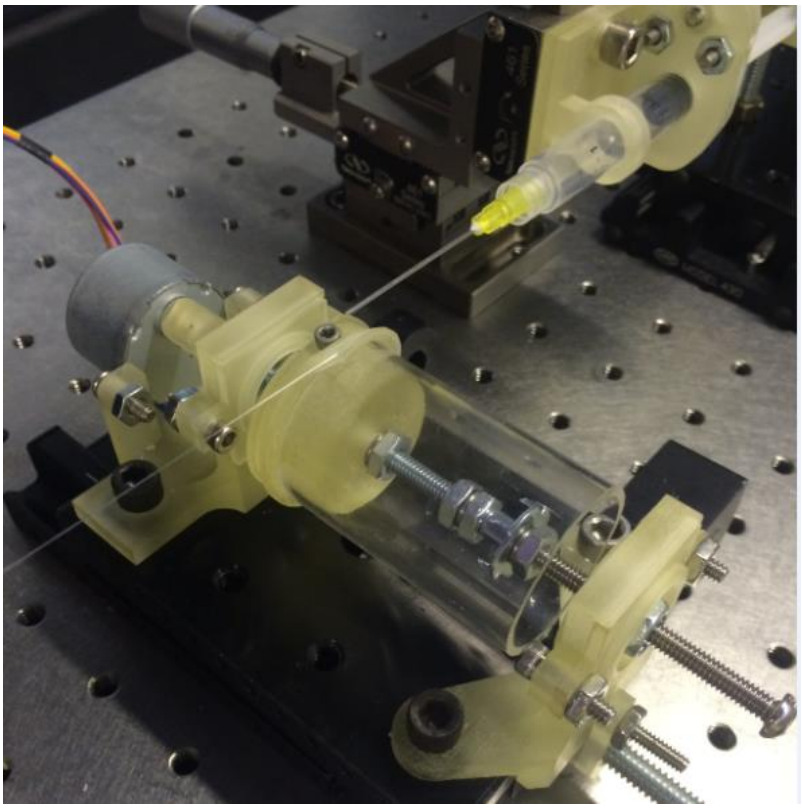

**Figure 12: Makeshift screw coupler, visible inside the acrylic spindle.**

Last, the fitment and mechanical principles of the epoxying device were tested. The spring loaded stage and motor carriage assembly was capable of driving the plunger through the syringe barrel on the 3-way adjustable fixture without issue. No tests were conducted to determine if the stepper's nut and bolt actuation scheme was capable of controlling this action, however the fitment and alignment of the motor carriage and the syringe barrel fixture were to specification.

## Measurement

Below are the results of the experiment for measuring absorption of the solar spectrum of an erbium doped fiber.

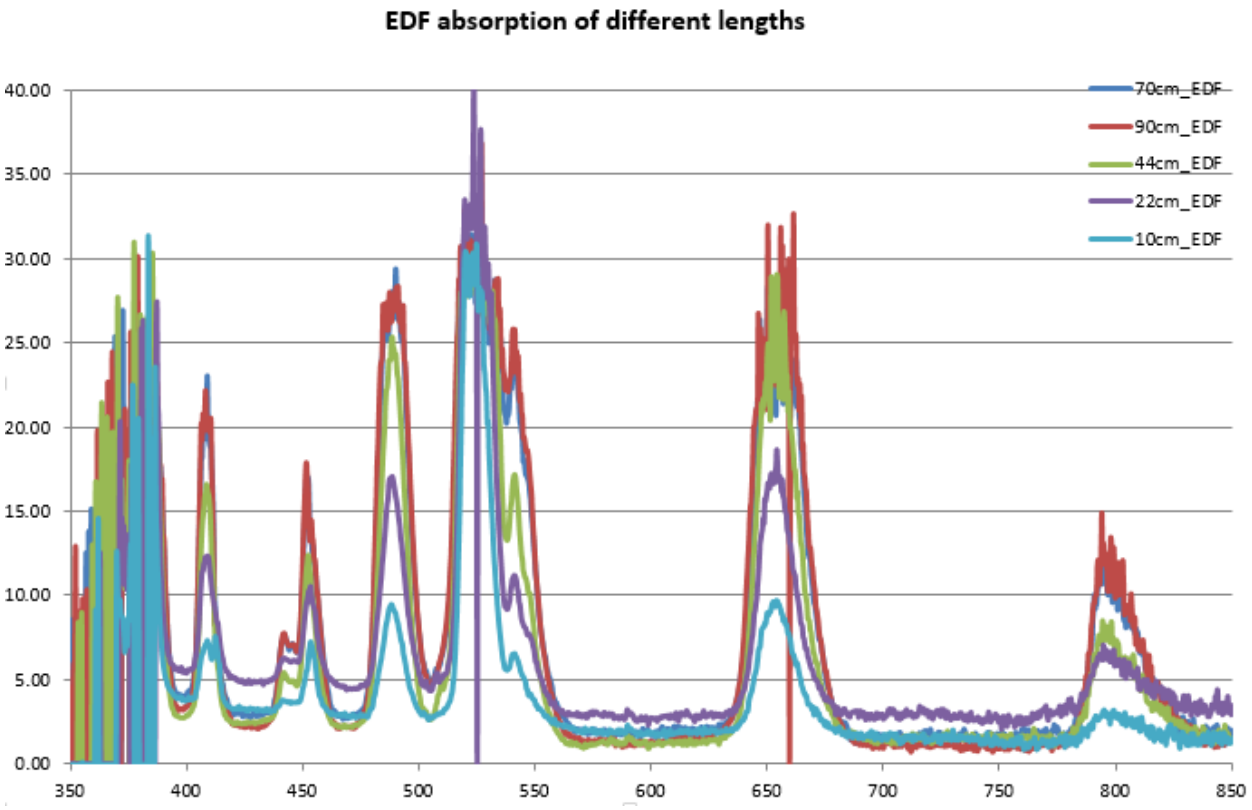


**Figure 13: Absorption bands of EDF**

Here we see there are six clear absorption bands across the solar spectrum at 405nm-415nm, 440nm-460nm, 480nm-500nm, 515nm-555nm, 640nm-675nm, and 785nm-815nm. This closely agrees with research by the Gwangju Institute of Science and Technology in South Korea, which states that there are six absorption bands: 405nm, 450nm, 490nm, 514nm, 532nm, and 650nm (Htein, Fan, Watekar, Han). The primary difference is that our data shows the 514 and 532 in a single peak, and also shows one from 785nm-815nm.

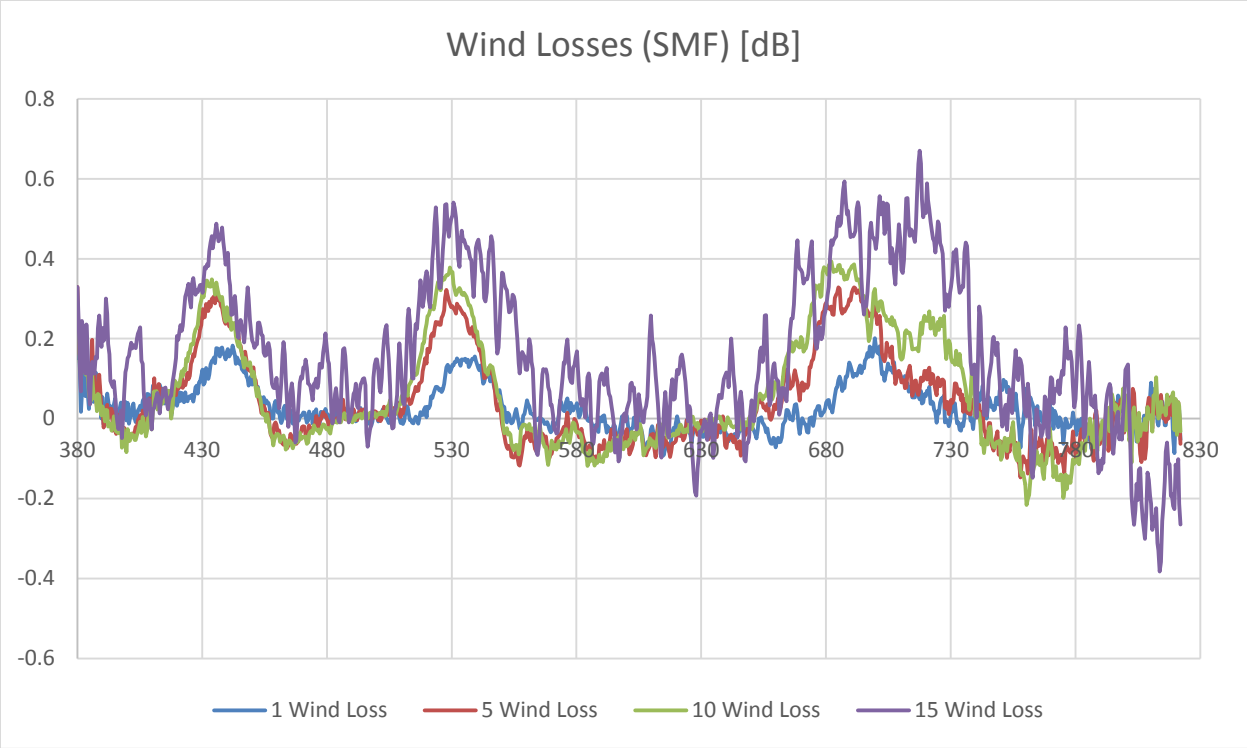


**Figure 14: Wind losses.**

This experiment revealed interesting behavior regarding losses caused by winding. Measured in dB, the first winding caused more or almost as much loss as the next four windings combined for most wavelengths. Then we see that wind loss increases only slightly going from five windings to ten windings. From ten to fifteen windings, the losses increase again, but in most wavelengths by less loss than the first winding created.

From this we can infer that the loss per wind decreases as we increase windings as the first windings create a kind of initial wind loss. A further study of the rate of change of loss with respect to windings can confirm this. Such a study was not conducted by our team, however, as the low losses as compared to the large absorption from the previous experiment shows that gain per unit wind, considering that each wind is barely over 10cm in length with some wavelengths

approaching 30dB absorption at that length, is much greater than loss per unit wind. At this point we have shown that amplification can be done, and better data could be gathered by creating a prototype coil and a reference coil and connecting it to the device under test position.

**Coupling**

While the fiber coil fabrication device was being developed, acrylic cylinders were used to find the best coupling method and the effectiveness of the coupling. Coupling was tested by coupling a <5mW purple laser pointer into the acrylic cylinder and acrylic dual-cylinder.

When the laser is perpendicularly or non-tangentially incident upon the cylinder, the light was both reflected back towards the source and passed through in a straight line with negligible refraction. The light that passed through in a straight line was spread out through refraction and beam widening.

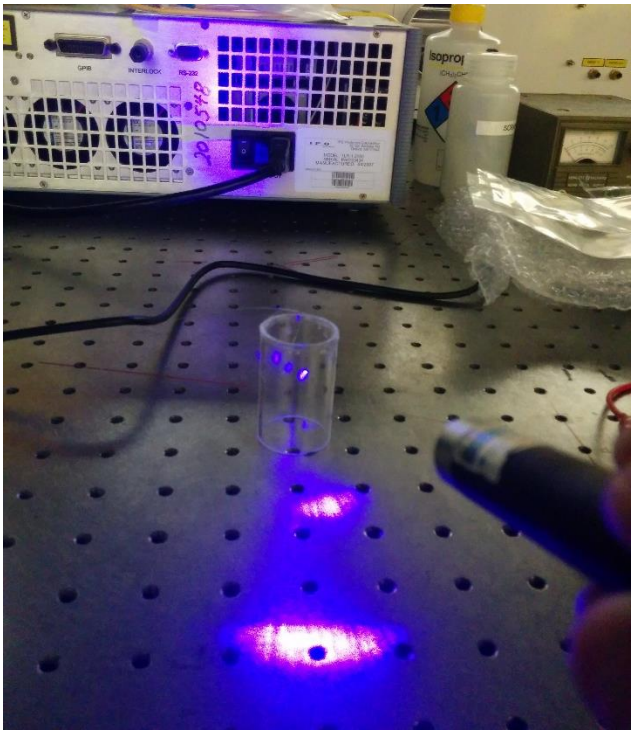

**Figure 15: Perpendicular insertion to single cylinder design**

When the laser is tangentially incident upon the acrylic, weak coupling was shown.

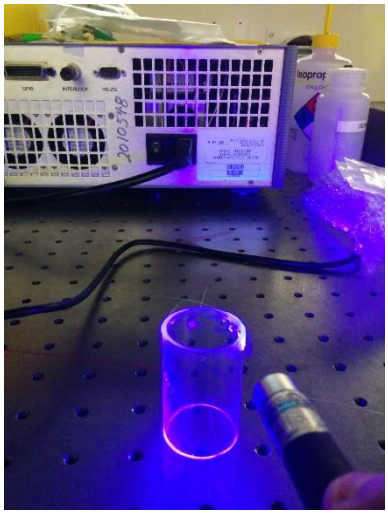

**Figure 16: Tangential insertion to single cylinder design**

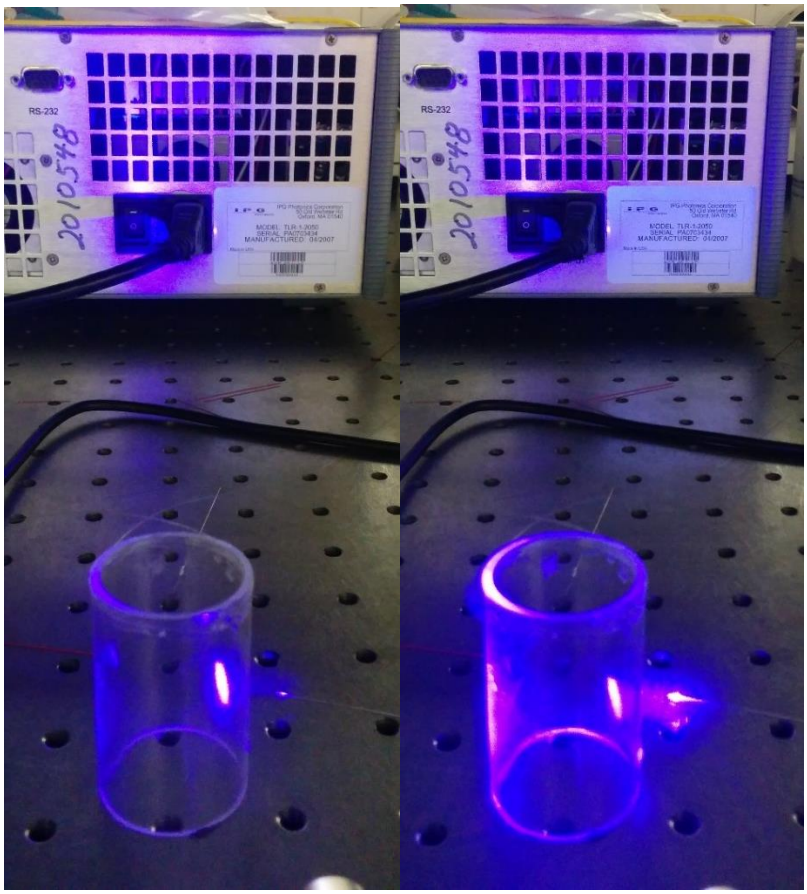


**Figure 17: Perpendicular and tangential insertion side-by-side.**

# CONCLUSION

This project resulted in far better, although different, results than originally imagined. Out of need for a way to build the fiber optic coil amplifier, we designed a cheap way to wind the fiber coils. Using components designed in SolidWorks that are 3D printed and assembled with motors, we have built a device that can wind fiber coils. Not only is this device useful for our intended purpose of winding a fiber optic coil amplifier, researchers at other universities are able to cheaply modify our design to their specifications and print and assemble it for other purposes, such as microfiber coil resonators or fiber optic gyroscopes.

With the data gathered from the measurements of the absorption and wind per unit loss of single mode fibers, we have shown that power amplification using the solar spectrum as a pump can be done. Coupling this with solar concentrators, alternative designs and alternative coupling mechanisms, solar power can be converted into a high energy laser.

Lastly, a prototype of our fiber optic coil amplifier has been successfully created from one of our winding device designs. This, combined with our measurements of absorption and loss, is a success that will be capitalized on in future research.

# REFERENCES


Htein, L., Fan, W., Watekar, P., and Han, W. (2012). *Amplification by white light-emitting diode pumping of large-core Er-doped fiber with 12 dB gain*. Opt. Lett., 37, 4853-4855.

Sumetsky, M. (2008). *Basic Elements for Microfiber Photonics: Micro/Nanofibers and Microfiber Coil Resonators*. Journal of Lightwave Technology, Vol. 26, No. 1, 1 January 2008

Arjmand, M., Ahmadi, V., Karimi, M. (2012). *Wavelength-Selective Optical Amplifier Based on Microfiber Coil Resonators.* Journal of Lightwave Technology, Vol. 26, No. 16, 15 August 2012